Integration of the Second Messenger c-di-GMP into the Chemotactic Signaling Pathway

Matthew H. Russell,[a] Amber N. Bible,[a] Xin Fang,[b] Jessica R. Gooding,[c] Shawn R. Campagna,[c] Mark Gomelsky,[b] Gladys Alexandre[a]

Department of Biochemistry, Cellular and Molecular Biology, University of Tennessee, Knoxville, Tennessee, USA[a]; Department of Molecular Biology, University of Wyoming, Laramie, Wyoming, USA[b]; Department of Chemistry, University of Tennessee, Knoxville, Tennessee, USA[c]

ABSTRACT **Elevated intracellular levels of the bacterial second messenger c-di-GMP are known to suppress motility and promote sessility. Bacterial chemotaxis guides motile cells in gradients of attractants and repellents over broad concentration ranges, thus allowing bacteria to quickly adapt to changes in their surroundings. Here, we describe a chemotaxis receptor that enhances, as opposed to suppresses, motility in response to temporary increases in intracellular c-di-GMP. *Azospirillum brasilense*'s preferred metabolism is adapted to microaerophily, and these motile cells quickly navigate to zones of low oxygen concentration by aerotaxis. We observed that changes in oxygen concentration result in rapid changes in intracellular c-di-GMP levels. The aerotaxis and chemotaxis receptor, Tlp1, binds c-di-GMP via its C-terminal PilZ domain and promotes persistent motility by increasing swimming velocity and decreasing swimming reversal frequency, which helps *A. brasilense* reach low-oxygen zones. If c-di-GMP levels remain high for extended periods, *A. brasilense* forms nonmotile clumps or biofilms on abiotic surfaces. These results suggest that association of increased c-di-GMP levels with sessility is correct on a long-term scale, while in the short-term c-di-GMP may actually promote, as opposed to suppress, motility. Our data suggest that sensing c-di-GMP by Tlp1 functions similar to methylation-based adaptation. Numerous chemotaxis receptors contain C-terminal PilZ domains or other sensory domains, suggesting that intracellular c-di-GMP as well as additional stimuli can be used to modulate adaptation of bacterial chemotaxis receptors.**

IMPORTANCE **To adapt and compete under changing conditions, bacteria must not only detect and respond to various environmental cues but also be able to remain sensitive to further changes in the environmental conditions. In bacterial chemotaxis, chemosensory sensitivity is typically brought about by changes in the methylation status of chemotaxis receptors capable of modulating the ability of motile cells to navigate in gradients of various physicochemical cues. Here, we show that the ubiquitous second messenger c-di-GMP functions to modulate chemosensory sensitivity of a bacterial chemotaxis receptor in the alphaproteobacterium *Azospirillum brasilense*. Binding of c-di-GMP to the chemotaxis receptor promotes motility under conditions of elevated intracellular c-di-GMP levels. Our results revealed that the role of c-di-GMP as a sessile signal is overly simplistic. We also show that adaptation by sensing an intracellular metabolic cue, via PilZ or other domains, is likely widespread among bacterial chemotaxis receptors.**

Received 4 January 2013 **Accepted** 14 February 2013 **Published** 19 March 2013

Citation Russell MH, Bible AN, Fang X, Gooding JR, Campagna SR, Gomelsky M, Alexandre G. 2013. Integration of the second messenger c-di-GMP into the chemotactic signaling pathway. mBio 4(2):e00001-13. doi:10.1128/mBio.00001-13.

Editor E. Peter Greenberg, University of Washington **Invited Editor** Caroline Harwood, University of Washington

Address correspondence to Gladys Alexandre, galexan2@utk.edu.

Motile bacteria detect changes in environmental conditions and respond by navigating toward niches that support optimal growth by chemotaxis (1). This behavior is widespread in various environments, and it is especially significant in soil bacteria (2). In chemotaxis, chemical cues are detected by dedicated receptors that relay information to the flagellar motors via a conserved signal transduction cascade (3). The model organism, *Escherichia coli*, possesses five chemotaxis receptors (Tar, Tsr, Tap, Trg, and Aer), and the sensory specificities for each of these receptors have been determined (4). Many bacterial species have a greater number of receptors than *E. coli* (5); however, their sensory specificity remains largely unknown.

Azospirillum brasilense is a motile alphaproteobacterium that possesses a single polar flagellum. Motile *A. brasilense* cells respond tactically not only by biasing the probability of changes in the swimming direction of the polar flagellum (changes in swimming reversal frequency, equivalent to "tumbles" of *E. coli*) but also by modulating transient increases in swimming velocity (6) (Fig. 1). The genome of *A. brasilense* encodes four chemotaxis pathways (7), with Che1 being the only experimentally characterized pathway (8). Aerotaxis (movement in oxygen gradients) is the strongest behavioral response in *A. brasilense* (9). In oxygen gradients, *A. brasilense* cells quickly navigate to a specific zone where the oxygen concentration is low, 3 to 5 μM, and optimal to support their preferred microaerobic metabolism that often involves oxygen-sensitive nitrogen fixation (10). Under conditions of high aeration, *A. brasilense* motile cells form clumps that are initially transient but become stable over time, with cells losing motility if high aeration conditions persist (8).

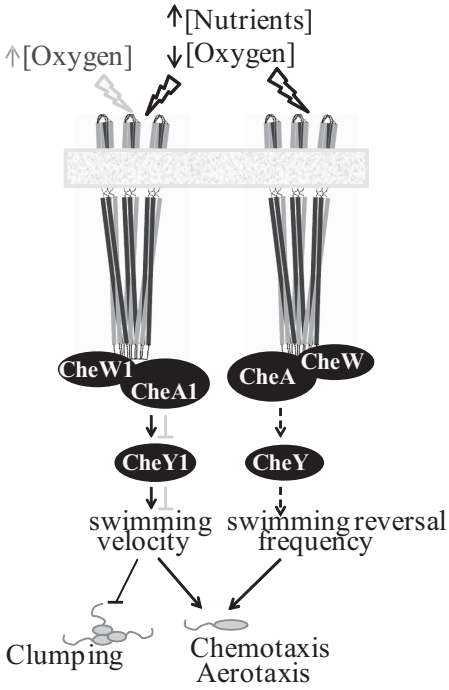

FIG 1 Cartoon summarizing the behaviors controlled by chemotaxis pathways in *A. brasilense*. The black and gray lines represent effects that occur under different environmental conditions represented at the top of the figure. The arrows represent interactions within chemotaxis proteins. Proteins of the Che1 pathway and proteins from another pathway are represented. Dashed lines represent putative interactions.

Most chemical stimuli are sensed indirectly in *A. brasilense* via net changes in intracellular energy levels (11). Chemo- and aerotactic responses to changes in energy metabolism have been identified in several bacterial species and are collectively referred to as "energy taxis" (5, 12). The behaviors controlled by chemotaxis pathways in *A. brasilense* are summarized in Fig. 1. An energy taxis receptor, AerC, has been previously shown to mediate the ability of motile *A. brasilense* cells to locate low-oxygen niches compatible with nitrogen fixation (13). An FAD bound to the sensory domain of AerC likely serves as a redox sensor (13). A transmembrane chemoreceptor, Tlp1, also functions in energy taxis. The sensory domain of Tlp1 is located in the periplasm and lacks a recognizable motif for redox or energy sensing, and thus the primary stimuli affecting Tlp1 remain unknown (14). Interestingly, Tlp1 contains a PilZ domain at its C terminus (15). PilZ domains are ubiquitous in bacterial genomes and are known to bind the bacterial second messenger c-di-GMP (16–18). The elevated intracellular c-di-GMP levels promote transition of motile cells to a sessile lifestyle (16–18), whereas aerotaxis or chemotaxis allows motile cells to further explore their surroundings (1). The unusual domain architecture of Tlp1 prompted us to investigate the unexpected interplay between chemotaxis and c-di-GMP.

RESULTS

Intracellular c-di-GMP content of cells varies in oxygen gradients. We began investigating the connection of c-di-GMP levels with chemotaxis by analyzing the behavior of the *A. brasilense chsA* mutant recently reported to be defective in chemotaxis (19). ChsA is an EAL domain protein predicted to have c-di-GMP phosphodiesterase (hydrolase) activity. Further, it has an N-terminal PAS domain that contains residues involved in heme binding (20), thus suggesting that oxygen regulates ChsA activity. We observed that the *chsA* mutant is impaired in motility in semisolid agar, which can be partially rescued by wild-type *chsA* provided in *trans* (Fig. 2A). Consistent with the assigned function of ChsA as a c-di-GMP phosphodiesterase, the *chsA* mutant had a greater steady-state intracellular c-di-GMP concentration than the wild type (Fig. 2B, before air removal/addition). We therefore expected that intracellular c-di-GMP levels in *A. brasilense* would respond to changes in aeration.

Unexpectedly, the intracellular c-di-GMP levels responded to air removal or addition in a highly dynamic fashion and fluctuated by more than 2-fold within 20 to 40 s of changes in aeration (Fig. 2B, wild type). The c-di-GMP levels in the *chsA* mutant and the wild type responded similarly to air removal. However, upon air addition, patterns of the c-di-GMP levels in the wild type and the *chsA* mutant differed. The most drastic difference between the two strains was detected 20 s after air addition, i.e., 6-fold-higher c-di-GMP levels in the mutant (Fig. 2B). We hypothesized that the aerotaxis and chemotaxis receptor Tlp1 containing the PilZ domain must be sensitive to such drastic changes in c-di-GMP levels. First, we investigated whether Tlp1 can bind c-di-GMP.

The PilZ domain of Tlp1 binds c-di-GMP. To test whether the PilZ domain of Tlp1 binds c-di-GMP, we fused the C-terminal PilZ domain of Tlp1 to MBP (see Fig. S1 in the supplemental material); purified the fusion protein, MBP-cTlp1; and analyzed, using equilibrium dialysis, its ability to bind c-di-GMP (21). MBP-cTlp1 bound c-di-GMP with an apparent K_d (dissociation constant) of 6.9 ± 1.2 μM (Fig. 3A). Given that only a fragment of Tlp1 was tested, it is possible that the K_d of the full-length Tlp1 is even lower, as reported for other PilZ domain receptors (17, 21). The binding capacity of MBP-cTlp1, B_{max}, calculated based on the equilibrium dialysis experiments, was 2.1 ± 0.1 mol c-di-GMP mol protein^{-1}. This suggests that the PilZ domain of Tlp1 can bind up to two molecules of c-di-GMP, similar to the known PilZ domain c-di-GMP receptors, *E. coli* YcgR (21) and *Pseudomonas putida* PP4397 (22).

While the apparent K_d value correlates well with the estimated intracellular c-di-GMP levels in the proteobacterial species, believed to be in the submicromolar-to-low-micromolar range (18), we also estimated actual intracellular concentrations in *A. brasilense* under the conditions of the temporal assay by liquid chromatography-tandem mass spectrometry (LC-MS/MS) by using a stable-isotope-labeled internal standard. The intracellular c-di-GMP concentrations in the wild type ranged from 2 to 4.5 μM when exposed to nitrogen gas and from 7.6 to 7.8 μM on air (Fig. 2B). These intracellular c-di-GMP concentrations are in the same range as the apparent K_d, which suggests that Tlp1 is capable of responding to changes in intracellular c-di-GMP concentrations. On the other hand, the intracellular c-di-GMP concentrations in the *chsA* mutant ranged from 7.4 to 17.7 μM, above the K_d value (with one exception at 4.1 M detected 10 s after air addition; Fig. 2B), suggesting that Tlp1 in the *chsA* mutant exists mostly in the c-di-GMP-bound state.

To investigate the mode of c-di-GMP binding by the PilZ domain of Tlp1, we mutagenized several conserved residues of the PilZ domain. c-di-GMP binding was abrogated in three of the constructed mutants, MBP-cTlp1$^{R562A\ R563A}$, MBP-cTlp1^{R567D}, and MBP-cTlp1^{N589A}, which contain mutations in three of the

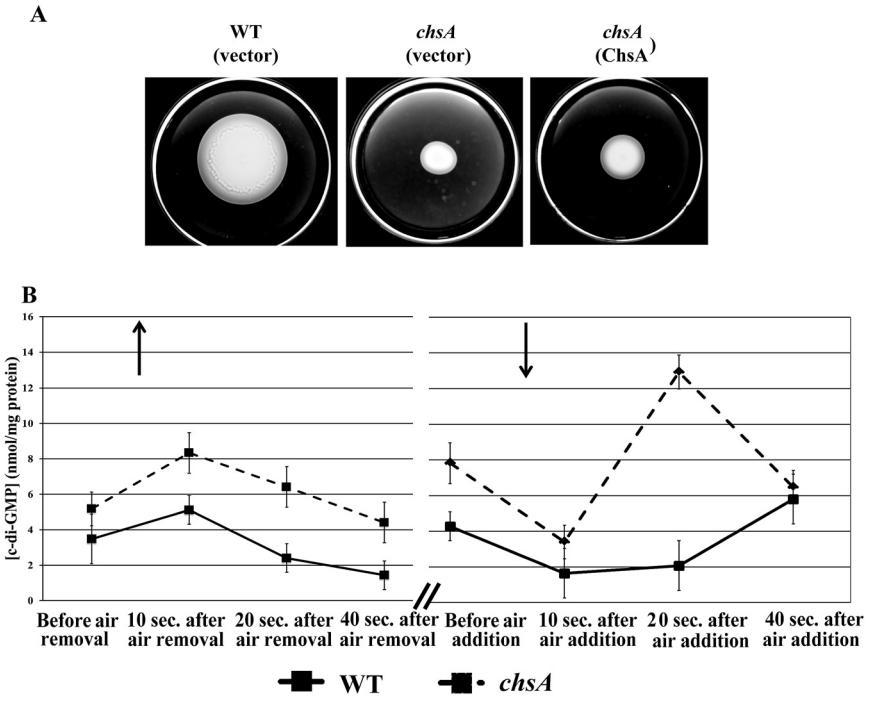

FIG 2 Rapid changes in intracellular c-di-GMP levels in *A. brasilense* upon changes in aeration. (A) Representative chemotaxis in semisoft agar plates with 0.5% (wt/vol) malate as a carbon source, 48 h postinoculation of *A. brasilense* Sp7 (wild type) and its *chsA* mutant derivative. The vectors used were pRK415 (vector) or pRKChsA (pRK415 expressing the c-di-GMP phosphodiesterase ChsA). All strains were motile. (B) Temporal changes in intracellular c-di-GMP concentrations in response to temporal changes in aeration in *A. brasilense* Sp7 and the *chsA* mutant. Air was bubbled in the cell suspensions for 5 min prior to the start of the experiment. Aliquots were taken at times indicated on the graph, and the concentration of c-di-GMP was analyzed via LC-MS/MS. Up and down arrows indicate air removal and air addition to the atmosphere of the cells, respectively. Slash bars indicate a time interval of approximately 5 min.

most conserved residues (R563, R567, N589) of the c-di-GMP binding loop, $Rx_3Rx_{20\text{-}30}D/NxSx_2G$ (15, 18, 21) (see Fig. S1 in the supplemental material). Another constructed mutant, MBP-cTlp1^{R562A}, with an alanine substitution in the nonconserved R562 residue located in the immediate vicinity of the c-di-GMP binding loop, showed lower capacity to bind c-di-GMP, with a K_d of 21.8 $\pm$ 7.1 μM (Fig. 3A), than the wild-type protein. The 3-fold decrease in c-di-GMP binding affinity observed in MPB-cTlp1^{R562A}, compared to that of MPB-cTlp1, suggests that residues near the conserved c-di-GMP binding consensus (15, 18, 21) can significantly influence c-di-GMP binding. In the following experiments, we will use Tlp1$^{R562A\ R563A}$ as well as Tlp1$^{\Delta PilZ}$, lacking a PilZ domain altogether, as variants that are completely unable to bind c-di-GMP. We will use Tlp1^{R562A} as a mutant protein partially impaired in c-di-GMP binding.

PilZ domain of Tlp1 affects aerotaxis responses. Having established the c-di-GMP binding ability of Tlp1, we explored its functional significance using aerotaxis assays. Aerotaxis can be detected in spatial gradients established in flat capillary tubes (10, 23). Under these conditions, *A. brasilense* forms an aerotactic band within 2 min at some distance from the meniscus, at the position in the gradient where metabolism is optimal (10). Cells within and outside the band remain motile, and the aerotactic band remains stable. As expected, the *tlp1* mutant was significantly affected in aerotaxis in that it formed an aerotactic band farther away from the meniscus than the wild type (Fig. 3B). Expression in the mutant of the wild-type Tlp1 in *trans* restored the proper band position (Fig. 3B). All of the Tlp1 variants that lacked (Tlp1$^{\Delta PilZ}$) or had mutated (Tlp1^{R562A} and Tlp1$^{R562A\ R563A}$) PilZ domains failed to fully rescue the *tlp1* mutant aerotaxis phenotype (Fig. 3B). We verified that these variants were expressed at levels comparable, albeit slightly elevated, to the levels of the wild-type Tlp1 (see Fig. S2 in the supplemental material). Consistent with their c-di-GMP binding capacities, the Tlp1^{R562A} protein partially complemented the aerotaxis defect of the mutant, while both Tlp1$^{\Delta PilZ}$ and Tlp1$^{R562A\ R563A}$ were completely inactive. Therefore, the ability to bind c-di-GMP via the PilZ domain is important for Tlp1 function in aerotaxis.

c-di-GMP binding to Tlp1 affects the ability of cells to increase swimming velocity in oxygen gradients. Transient changes in both swimming velocity and reversal frequency are hallmarks of the *A. brasilense* aerotaxis response (6). While transient changes in the swimming velocity are controlled by Che1, the identity of the chemotaxis pathway(s) controlling transient changes in the swimming reversal frequency remains unknown (6). To investigate whether c-di-GMP affects swimming velocity versus reversal frequency, we used the temporal oxygen gradient assay, where a sudden decrease or increase (air removal or addition) in aeration makes readily detectable changes in the locomotor behavior (6, 9, 14). The wild type responded to air removal and addition by significantly increasing the swimming velocity, before returning to prestimulus swimming velocity, after over 2 min (Fig. 4A). The *tlp1* mutant also responded by transiently increasing swimming velocity upon air removal but not air addition (Fig. 4B). Further, the time of increased swimming velocity upon air addition for the *tlp1* mutant was much shorter than that of the wild type (Fig. 4B). Expressing wild-type Tlp1 in the *tlp1* mutant background restored the wild-type swimming velocity response pattern and time (Fig. 4C).

When the Tlp1$^{R562A\ R563A}$ variant, which is completely impaired in c-di-GMP binding, was expressed in the *tlp1* mutant, the cells were unable to significantly increase swimming velocity upon air removal or air addition (Fig. 4F). Cells expressing either Tlp1^{R562A} with partial ability to bind c-di-GMP or Tlp1$^{\Delta PilZ}$ lacking the PilZ domain responded to air removal by decreasing the swimming velocity, an inverted response compared to that of the wild type (Fig. 4D and E). Further, the strain expressing Tlp1^{R562A} responded to air removal by swimming slower, ~15 s after the initial stimulus, which suggests a significant defect in the receptor's sensitivity (Fig. 4E). Cells expressing Tlp1$^{\Delta PilZ}$ were unable to respond to air addition, which was similar to the behavior of the *tlp1* mutant (Fig. 4B and D). On the other hand, the *tlp1* mutant

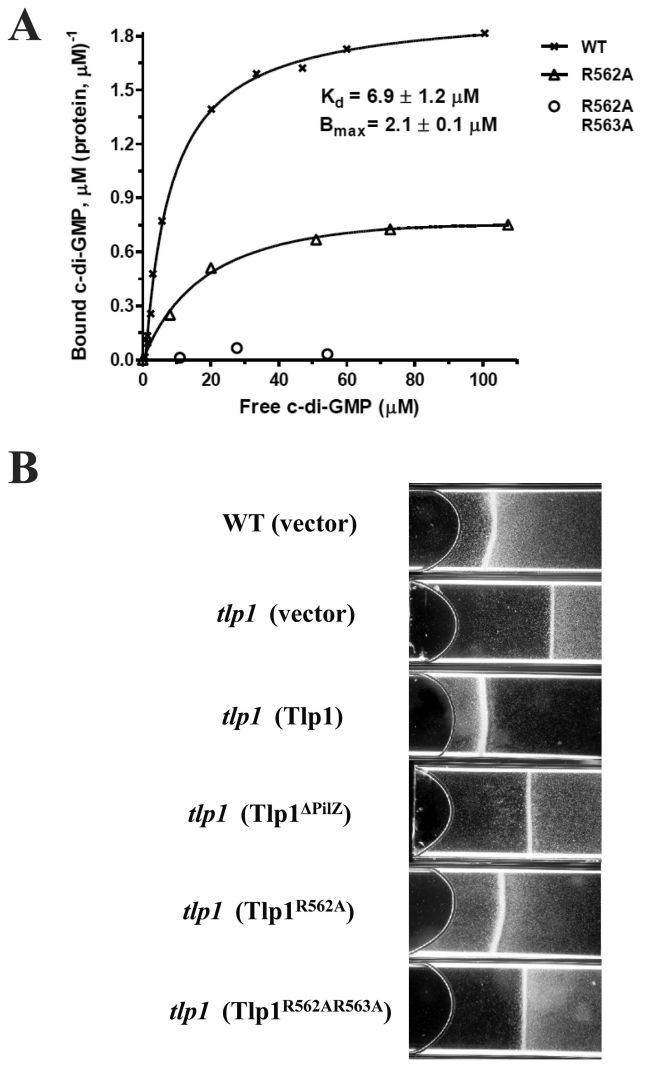

FIG 3 c-di-GMP binding to Tlp1 and its mutant variants and effects of c-di-GMP binding on aerotaxis. (A) Saturation plot of equilibrium binding between cTlp1 and c-di-GMP. c-di-GMP was injected into 1 cell of a dialysis cassette, while MBP-cTlp1 protein or its mutant variants, MBP-cTlp1^{R562A}, MBP-cTlp1$^{R562A\ R563A}$, MBP-cTlp1^{R567D}, and MBP-cTlp1^{N589A}, were injected into the opposite cell, separated by a membrane with a 10-kDa cutoff. Concentrations of free and protein-bound c-di-GMP were measured following the establishment of an equilibrium. MBP-cTlp1$^{R562A\ R563A}$, MBP-cTlp1^{R567D}, and MBP-cTlp1^{N589A} showed no detectable c-di-GMP binding; data for only one nonbinding protein, MBP-cTlp1$^{R562A\ R563A}$, are shown. (B) Spatial aerotaxis mediated by Tlp1, Tlp1$^{\Delta PilZ}$, Tlp1^{R562A}, and Tlp1$^{R562A\ R563A}$. Motile cell suspensions were adjusted to equivalent cell density. Within 2 min, the wild-type *A. brasilense* Sp7 formed an aerotactic band at a distance from the meniscus (air/liquid interface) where the dissolved oxygen concentration is optimum for energy production (10). SG323 (the *tlp1* mutant), pRK415 (vector), pRKTlp1 (pRK415 expressing Tlp1), pRKTlp1$^{\Delta PilZ}$ (Tlp1$^{\Delta PilZ}$), pRKTlp1^{R562A} (Tlp1^{R562A}), and pRKTlp1$^{R562A\ R563A}$ (Tlp1$^{R562A\ R563A}$).

expressing Tlp1^{R562A} increased swimming velocity upon air addition, but this response was significantly delayed (~7 s) (Fig. 4E), again suggesting that poor ability to bind c-di-GMP alters the sensitivity of Tlp1 to the aeration stimulus. Further, cells expressing Tlp1$^{\Delta PilZ}$ (but not Tlp1^{R562A} or Tlp1$^{R562A\ R563A}$) swam significantly faster than other strains (Fig. 4D), which indicates that they are unable to maintain a steady-state swimming velocity. This phenotype, together with the response patterns of the Tlp1 variants that range from changes in sensitivity to inverted responses, strongly suggest that c-di-GMP modulates the sensitivity of Tlp1 and thus its ability to process sensory signals (aeration). In this regard, the role of the c-di-GMP binding PilZ domain is similar to the role played by adaptation proteins CheB and CheR in *E. coli* (1, 4, 24).

c-di-GMP binding to Tlp1 affects the ability of cells to decrease swimming reversal frequency in oxygen gradients. Decreased or increased aeration caused the wild-type *A. brasilense* cells not only to swim faster for a short time (increased swimming velocity) but also to suppress changes in the swimming direction (reduced swimming reversal frequency), before adapting to new conditions (6, 14). The *tlp1* mutant responded to air removal by reducing the swimming reversal frequency, with a pattern not significantly different ($P < 0.05$) from the response of the wild type (Fig. 5A). A similar response was observed in the *tlp1* mutant complemented with the wild-type Tlp1 (Fig. 5A).

Surprisingly, when Tlp1$^{\Delta PilZ}$, Tlp1^{R562A}, or Tlp1$^{R562A\ R563A}$ were expressed in the *tlp1* mutant, the cells responded to air removal by briefly (~10 s) increasing the swimming reversal frequency, before adapting to the new aeration conditions (Fig. 5A). This inverse response suggests that c-di-GMP affects processing of the stimulus (changes in aeration) by controlling the frequency of changes in the swimming direction. Furthermore, when Tlp1$^{R562A\ R563A}$ was expressed in the *tlp1* mutant, the cells drastically decreased the steady-state swimming bias (0.07 cell^{-1} s^{-1}), i.e., they swim more "smoothly" relative to the wild type (0.4 cell^{-1} s^{-1}) (Fig. 5A). These results confirm the notion made earlier that c-di-GMP binding modulates the sensitivity of Tlp1 to changes in aeration.

Upon air addition, the wild type decreased the swimming reversal frequency for ~30 s before adapting and returning to a steady-state swimming behavior (0.6 cell^{-1} s^{-1}) (Fig. 5B). In contrast, the *tlp1* mutant did not immediately respond to air addition; instead, the swimming reversal frequency decreased gradually (Fig. 5B). The *tlp1* mutant complemented with Tlp1 had the wild-type response to air addition (Fig. 5B). Tlp1 thus contributes most to aerotaxis upon increased aeration, which parallels the increase in intracellular c-di-GMP content. The *tlp1* mutant expressing Tlp1$^{\Delta PilZ}$, Tlp1^{R562A}, or Tlp1$^{R562A\ R563A}$ responded to air addition by increasing the swimming reversal frequency, i.e., the opposite response compared to that of the wild type (Fig. 5B).

These results establish that c-di-GMP binding to the PilZ domain of Tlp1 is critical for proper changes in swimming reversal frequency. Taken together with the results described in the previous section, they suggest that c-di-GMP affects both swimming velocity and reversal frequency. How is this possible if these processes have been shown to be controlled by different Che pathways? To address this question, we explored the possibility that Tlp1 signals via more than one Che pathway.

Tlp1 signals via Che1 and another Che pathway. The Che1 pathway in *A. brasilense* directly controls increases in swimming velocity upon changes in aeration. To test if c-di-GMP binding to Tlp1 modulates Che1 activity, we analyzed aerotaxis in a *che1* mutant and a *che1 tlp1* double mutant under conditions where Tlp1 is most active, i.e., aerotaxis in response to increases in aeration conditions (Fig. 5B). Consistent with previous results, the *che1* mutant and the *che1 tlp1* double mutant did not respond to air addition by increasing swimming velocity (see Fig. S3 in the

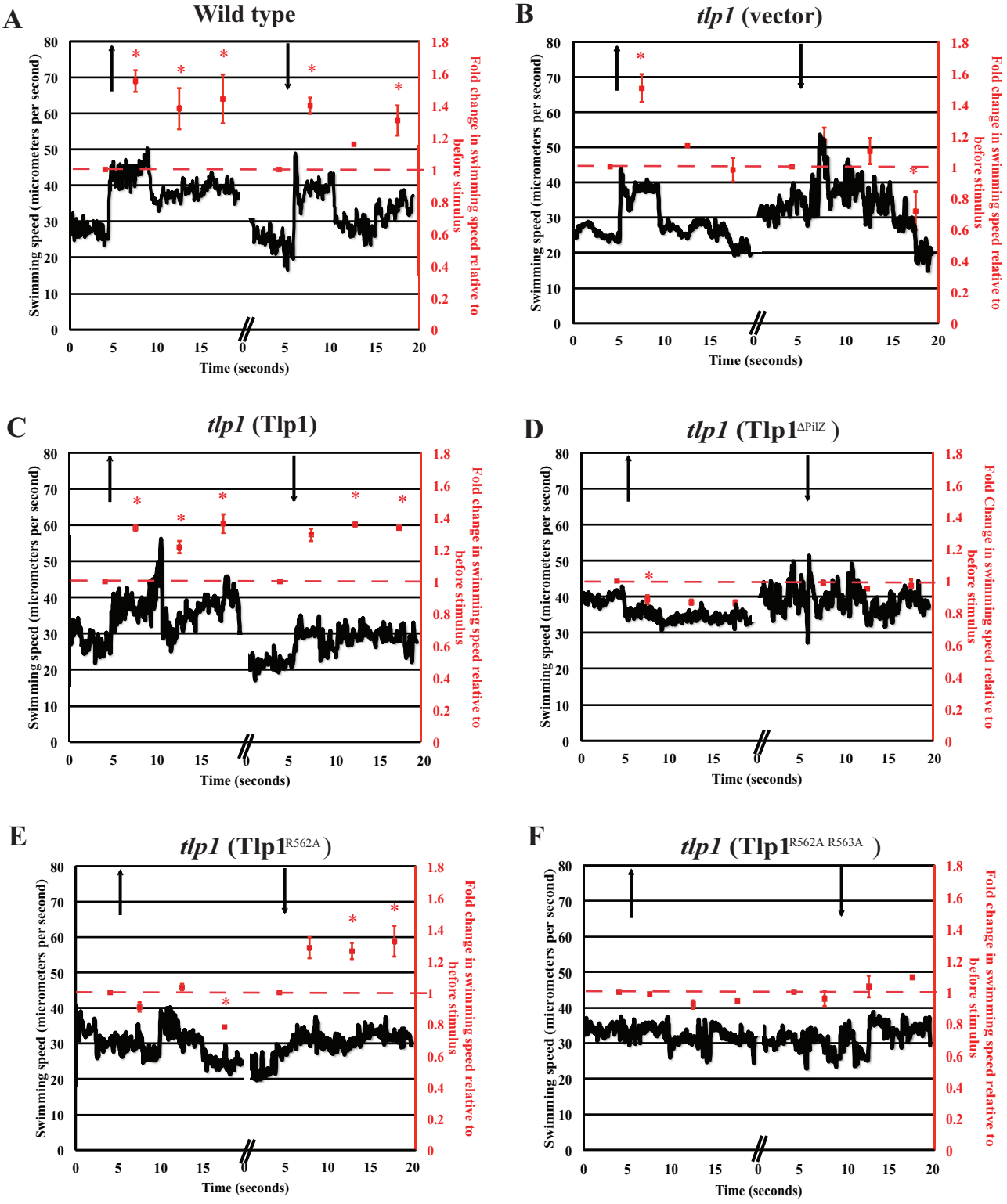

FIG 4 Effects of mutations in Tlp1 on swimming velocity upon changes in aeration. A suspension of motile cells was analyzed for temporal changes in swimming velocity upon air removal (arrow pointing up) and air addition (arrow pointing down) by motion-tracking analysis from video segments recorded during the assay. Cells were equilibrated 6 min prior to air removal and air addition. Left axis, the average swimming velocity of all motile cells frame by frame over 20-s intervals around the time of air removal and air addition was analyzed by GraphPad (Prism). Right axis, fold change in swimming velocity in 5-s intervals relative to before air removal and air addition. The dashed red line indicates average prior to stimulus, and asterisk indicates a significant departure from before stimulus with a confidence level of 0.05. Strains and plasmids are the same as described for Fig. 3B.

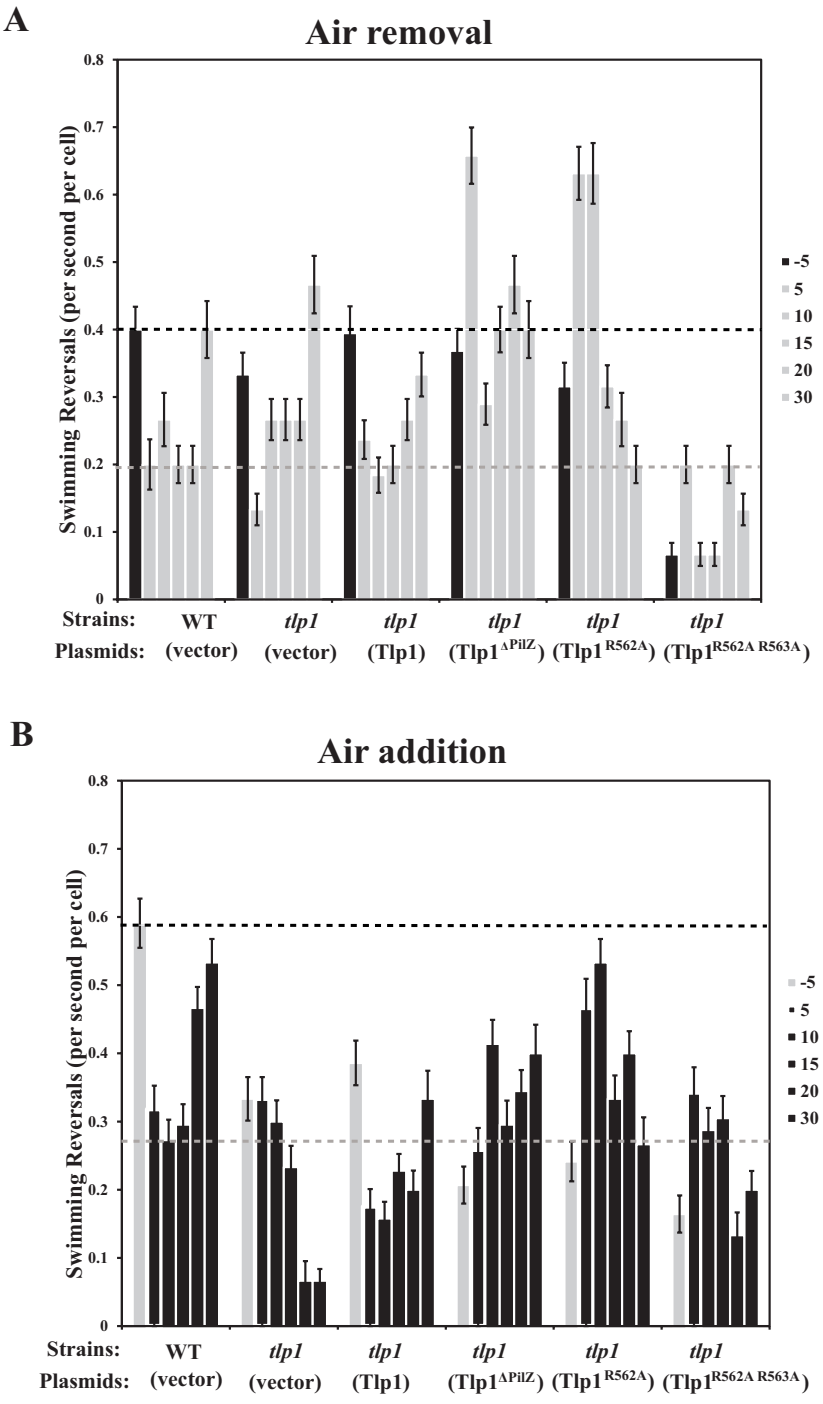

FIG 5 Effects of mutations in Tlp1 on swimming reversal frequency upon changes in aeration. The swimming reversal frequency was determined as the average number of changes in the swimming direction per second and per cell calculated from video images recorded during the assay and analyzed as 30-frame segments (taken in 1 s), using ImageJ software. The cells were equilibrated for 5 min in air prior to air removal (A) or in pure N_2 atmosphere prior to air addition (B). The black dashed horizontal line indicates swimming reversal frequency of the wild type under steady-state conditions (i.e., before stimulus and after adaptation). The gray dashed horizontal line indicates minimum reversal swimming frequency of the wild-type strain during the response. Bars indicate time before (−5 s) and after (5, 10, 15, 20, and 30 s) air removal. Black bars indicate cell suspension in air, and gray bars indicate cell suspensions in N_2.

supplemental material). Expressing the wild-type Tlp1 (or any of the Tlp1 mutant variants) in the *che1 tlp1* double mutant did not restore the swimming velocity response (see Fig. S3). Therefore, we conclude that Tlp1 modulates transient changes in swimming velocity during aerotaxis via the Che1 pathway.

We compared reversal frequencies in the *che1* and *che1 tlp1* mutants (Table 1). The reversal frequency of the *che1* mutant (0.07 ± 0.02 $cell^{-1}$ s^{-1}) was much lower than that of the wild type (0.43 ± 0.05 $cell^{-1}$ s^{-1}), but unlike the wild type, its reversal frequency did not change upon air addition (Table 1). This is similar to the lack of response of a *tlp1* mutant strain (compare with Fig. 5). The double *che1 tlp1* mutant had an intermediate (0.27 ± 0.03 $cell^{-1}$ s^{-1}) steady-state reversal frequency between that of the *che1* and the *tlp1* (0.33 ± 0.03 $cell^{-1}$ s^{-1}) strains, and its reversal frequency did not change upon air addition, i.e., there was no response to air addition. The *che1 tlp1* mutant expressing Tlp1 in *trans* responded similar to the wild type. These results strongly suggest that Tlp1 regulates swimming reversal frequency independent of the Che1 pathway; therefore, Tlp1 must signal via more than one Che pathway.

When $Tlp1^{R562A\ R563A}$ was expressed in the *che1 tlp1* double mutant, air addition evoked a transient decrease in the reversal frequency that was mostly similar to the wild-type response. On the other hand, the *che1 tlp1* cells expressing either $Tlp1^{\Delta PilZ}$ or $Tlp1^{R562A}$ were no longer able to respond to air addition (Table 1). Therefore, Tlp1 variants impaired in c-di-GMP binding no longer regulate swimming reversal frequency via the second, Che1-independent, Che pathway.

Increased c-di-GMP concentration promotes clumping and attachment of cells lacking Tlp1. Cultures of the *chsA* mutant formed stable clumps, regardless of the growth conditions (Fig. 6A), suggesting that clumping is caused, at least in part, by increased intracellular c-di-GMP levels in this mutant (Fig. 2B). Clumping and swimming motility are inversely regulated in *A. brasilense*, with clumps being formed under conditions of high oxygen (8, 14).

When grown at high aeration, the *tlp1* mutant expressing $Tlp1^{\Delta PilZ}$, $Tlp1^{R562A}$, or $Tlp1^{R562A\ R563A}$ clumped significantly more than the wild type or *tlp1* mutant (Table 2). Similarly, the *tlp1* mutant as well as the *tlp1* mutant expressing $Tlp1^{\Delta PilZ}$ or $Tlp1^{R562A\ R563A}$ formed clumps that remained at the position of the initial aerotactic band as the band moved farther away from the meniscus (Fig. 6B). These results suggest that the inability to bind c-di-GMP correlates with the loss of sensitivity to the oxygen gradient and thus produces a defective aerotactic response (Fig. 6B). In addition to forming more

TABLE 1 Swimming reversal frequency upon air addition in the temporal aerotaxis assay

Strain	Prestimulus N_2 frequency	Response to air addition[b]	
		Reversal frequency (reversal per s)	Adaptation
WT (vector)	0.43 ± 0.05	0.29 ± 0.03[a]	Yes
che1 mutant	0.07 ± 0.02	0 (NR)	NA
che1 tlp1 mutant (vector)	0.27 ± 0.03	0.2 ± 0.03 (NR)	NA
che1 tlp1 mutant (pRKTlp1)	0.4 ± 0.04	0.07 ± 0.02[a]	Yes
che1 tlp1 mutant (pRKTlp1$^{\Delta PilZ}$)	0.13 ± 0.02	0.13 ± 0.02 (NR)	NA
che1 tlp1 mutant (pRKTlp1^{R562A})	0	0.07 ± 0.02 (NR)	NA
che1 tlp1 mutant (pRKTlp1$^{R562A\ R563A}$)	0.48 ± 0.04	0.22 ± 0.03[a]	Yes

[b] NR, no response; NA, not applicable.

[a] Statistically different from the steady-state swimming reversal frequency prior to air addition.

clumps, the *tlp1* mutant or the *tlp1* mutant expressing Tlp1$^{\Delta PilZ}$, Tlp1^{R562A}, or Tlp1$^{R562A\ R563A}$ also formed more biofilms on abiotic surfaces than the wild type or the *tlp1* mutant complemented with Tlp1 (Fig. 6C). Therefore, c-di-GMP binding to Tlp1 promotes aerotaxis by increasing swimming velocity and decreasing reversal frequency and also prevents or delays transition of cells to a sessile lifestyle, which leads to clumps or biofilms on abiotic surfaces.

DISCUSSION

In this study, we demonstrated how the second messenger c-di-GMP is used by an *A. brasilense* energy taxis receptor Tlp1 as an intracellular signal for optimizing responses to changes in oxygen concentration during aerotaxis. We showed, for the first time, that sudden changes in aeration affect intracellular c-di-GMP levels quickly (within seconds) and to a substantial degree (Fig. 2B). The aerotaxis receptor Tlp1, whose primary sensory mode remains unknown, monitors these fast changes in intracellular c-di-GMP to adjust its sensitivity to oxygen. These results also show that c-di-GMP binding to Tlp1 affects both swimming velocity and reversal frequency, respectively, via Che1 and another, yet unidentified, Che pathway (Fig. 7).

At the mechanistic level, c-di-GMP binding to the C-terminal PilZ domain of Tlp1 is predicted to cause significant conformational changes, as has been shown for other PilZ domain receptors whose structures have been solved in the presence and absence of c-di-GMP (25, 26). The c-di-GMP-induced conformational changes may affect Tlp1 interactions with the downstream chemotaxis signaling complex and/or with other chemotaxis receptors that are known to form mixed multireceptor arrays (27–32).

The data showing that Tlp1 mutants are impaired in c-di-GMP binding suggest that c-di-GMP controls the sensitivity of Tlp1 to the oxygen changes and the ability to process the signal. These parameters are usually controlled by chemotaxis adaptation proteins. In *E. coli*, the adaptation proteins methyltransferase CheB and methylesterase CheR (24) reset sensitivity of each chemoreceptor by regulating its methylation status (33). At present, there is no evidence that Tlp1 is modified by differential methylation. Further, temporal responses to oxygen in *A. brasilense* do not appear to involve adaptation by differential methylation (34). Here, we have observed that c-di-GMP binding to Tlp1 mediates sensory adaptation under conditions of elevated intracellular c-di-GMP (Fig. 7). Methylation-independent adaptation has been proposed for other energy taxis receptors (35–37), and we suggest that c-di-GMP binding represents a new adaptation mechanism. Whether it acts in place of methylation-dependent adaptation or in addition to it remains to be investigated.

Tlp1 is a major, but not the only, receptor that mediates energy taxis in *A. brasilense* (13, 14). What makes it particularly suitable for responding to changes in intracellular c-di-GMP? We speculate that the answer may lie in the prominent role that Tlp1 plays in chemo- and aerotaxis in *A. brasilense*. The lack of Tlp1 causes aerotaxis and chemotaxis defects under all conditions tested (14). In this regard, the phenotype of the *tlp1* mutant is similar to the phenotypes of strains carrying mutations in the most abundant *E. coli* receptors, whose impairment affects the steady-state swimming reversal frequency under various growth conditions (30, 38–40). The highly abundant receptors Tar and Tsr of *E. coli* are primarily responsible for sensory adaptation (41–43), and Tlp1 appears to belong to the same category of chemoreceptors. Therefore, enabling Tlp1 with c-di-GMP sensing allows cells to coordinate locomotor response sensitivity under various conditions. While we showed here that c-di-GMP levels respond quickly to changes in oxygen tension and that the c-di-GMP phosphodiesterase ChsA may contribute to these changes, it is likely that changes in other environmental stimuli important for *A. brasilense* also result in fast changes in intracellular c-di-GMP. Like many proteobacteria, the *A. brasilense* genome contains numerous enzymes involved in c-di-GMP synthesis and hydrolysis that appear to monitor diverse environmental stimuli (7). Therefore, we predict that intracellular c-di-GMP levels affect chemotactic behavior in response to various stimuli.

Data obtained here have an important implication for the prevalent paradigm that elevated intracellular c-di-GMP levels suppress motility and promote sessility (16, 18, 44–46). On the one hand, *A. brasilense* conforms to this paradigm, i.e., elevated c-di-GMP levels (e.g., in the *chsA* mutant) promote sessility as evidenced by the increased clumping and improved cell attachment to surfaces. On the other hand, temporary spikes in c-di-GMP levels sensed by Tlp1 promote motility by increasing swimming velocity and decreasing reversal frequency instead of inhibiting it. Therefore, the static view of intracellular c-di-GMP levels as a deterministic factor in bacterial behavior is clearly overly simplistic. The highly dynamic nature of c-di-GMP signaling, as observed here and reported by other groups (18, 47), makes c-di-GMP a well-suited intracellular cue to integrate information from multiple inputs into regulation of the locomotor behavior. How common is such integration?

An analysis of the protein domain architectures of 20,681 chemotaxis receptors (Pfam database [48]) indicates that 52 of these proteins, primarily from the proteobacterial species, contain C-terminal PilZ domains (Fig. 8). Therefore, c-di-GMP-mediated chemoreceptor adaptation is clearly not unique to *A. brasilense*.

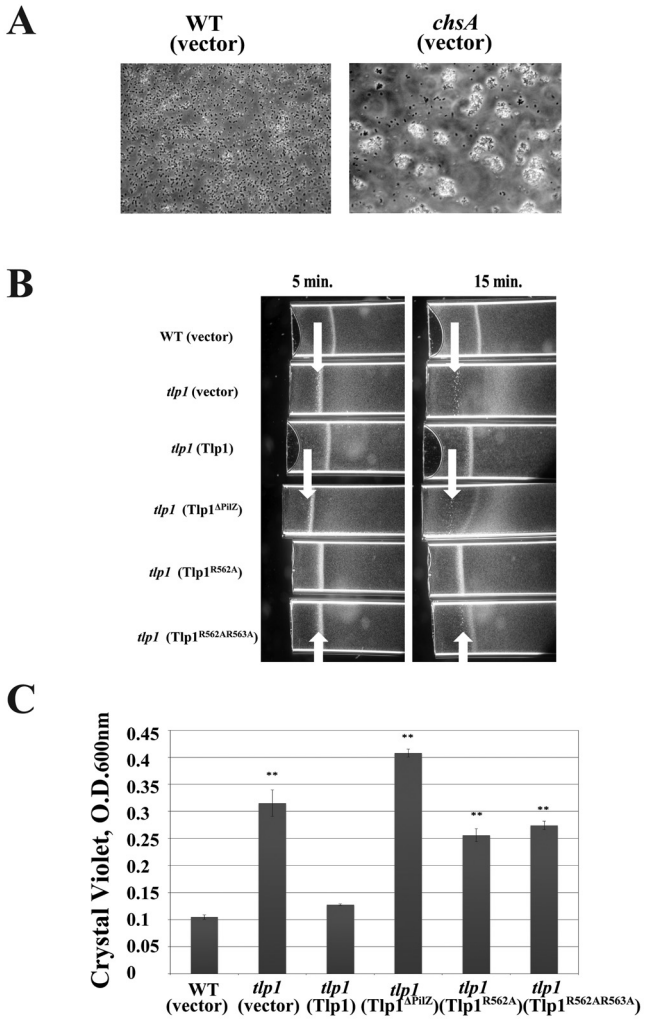

FIG 6 Elevated intracellular c-di-GMP affects the transition from free-swimming to sessile lifestyle in *A. brasilense*. (A) Representative images demonstrating cell behavior as observed in cultures grown under conditions of high aeration and at high cell densities (late exponential phase), in minimal medium supplemented with ammonium and pyruvate as the nitrogen and carbon sources, respectively, in *A. brasilense* Sp7 (left) and its *chsA* mutant (right). Plasmids are the same as those described in the legend to Fig. 2A. (B) Aerotaxis band formation in *A. brasilense* Sp7 and its *tlp1* derivative after 5 min (left) or 15 min (right) of incubation. Areas of clumped cell accumulation are indicated by an arrow. Strains and plasmids are the same as described for Fig. 3B. (C) Biofilm formation of *A. brasilense* Sp7 and its *tlp1* mutant after a 3-day incubation in microtiter plates containing MMAB. Biofilm levels were quantified by the absorbance (OD_{600}) of crystal violet-stained material recovered from polystyrene surfaces (58). Statistically significant differences are indicated by two asterisks ($P < 0.005$).

The influence of c-di-GMP on chemotaxis receptors may be even broader if one assumes that some chemoreceptors interact with stand-alone PilZ domain proteins, which are abundant in bacterial genomes (15–18). Further, several hundred chemotaxis receptors contain non-PilZ domains C-terminal of the methyl accepting protein (MCP) domains, suggesting that integration of inputs from c-di-GMP and other signaling molecules may represent a widespread mechanism for adapting sensitivity of chemotaxis receptors.

TABLE 2 Clump fractions of *A. brasilense* Sp7 and *tlp1* mutant derivatives under conditions of growth with high aeration

Strain	Clump fraction[a]	*P* value
WT (vector)	0.09 ± 0.002	
tlp1 mutant (vector)	0.08 ± 0.002	0.07
tlp1 mutant (Tlp1)	0.06 ± 0.002	0.0005
tlp1 mutant ($Tlp1^{\Delta PilZ}$)	0.18 ± 0.001	0.0003
tlp1 mutant ($Tlp1^{R562A}$)	0.19 ± 0.01	0.0005
tlp1 mutant ($Tlp1^{R562A\ R563A}$)	0.16 ± 0.01	0.0006

[a] The clump fraction is defined as the number of clumps relative to the total number of free-swimming cells.

MATERIALS AND METHODS

Media, bacterial strains, and growth conditions. *A. brasilense* Sp7, a wild-type strain, and its *tlp1* mutant, SG323 (14), were used throughout this study. Bacterial strains and plasmids are described in Table S1 in the supplemental material. *A. brasilense* strains were grown in TY rich medium (10 g tryptone $liter^{-1}$, 5 g yeast extract $liter^{-1}$) with the appropriate antibiotics or minimal medium for *A. brasilense* (MMAB) (49), at 28°C with shaking. *E. coli* strains were grown in LB at 37°C with the appropriate antibiotics. The biofilm assay was performed using crystal violet (50). For the flocculation assay, cells were grown overnight at 28°C with shaking in TY medium to an optical density at 600 nm (OD_{600}) of 1.1 to 1.3 and then inoculated into 5 ml MMAB supplied with 0.5 mM sodium nitrate and 8 mM fructose as the nitrogen and carbon sources, respectively, as described previously (14). The fraction of flocculation was calculated as described (8).

Site-specific mutations and complementation. For complementation, *tlp1* (GenBank accession number AY584240) and 737 bp upstream of the start codon were PCR amplified from genomic DNA with primers Tlp1HindIII-F and Tlp1XbaI-R1 (see Table S2 in the supplemental material). The PCR product was digested with HindIII and XbaI and cloned into pUC19 to yield pUCTlp1 (see Table S1). The HindIII/XbaI fragment of pUCTlp1 was ligated into a broad-host-range vector, pRK415, resulting in pRKTlp1. pUCTlp1 was used to construct $tlp1^{\Delta PilZ}$ by PCR amplification with primers Tlp1HindIII-F and Tlp1XbaI-R2 (see Table S2), digestion with HindIII and XbaI, and ligation into pRK415 (51) to yield pRK-pilZ. Both constructs were introduced into *A. brasilense* SG323 by triparental mating using pRK2013 as a helper (52). For site-directed mutagenesis, codons were replaced using pUCTlp1 as the template and the QuikChange II kit (Stratagene). The mutated *tlp1* versions were cloned into plasmid pRK415 as described for the wild-type *tlp1*. The primers used for site-directed mutagenesis are listed in Table S2.

Behavioral assays. The soft agar assay was performed by incubating liquid cultures in MMAB with shaking overnight at 28°C. The optical density of the cultures was standardized, and 5 μl was inoculated into 0.3% MMAB. Plates were incubated 48 h at 28°C. Spatial aerotaxis assays were performed in a perfused chamber as previously described (9). Over 95% of cells were motile within the cell suspension prepared. In this assay, the wild-type strain formed an aerotactic band within 2 min.

For the temporal aerotaxis assay, a 10-μl drop of motile cells suspended in MMAB supplied with 10 mM pyruvate as a carbon source was placed in a chamber in which the humidified gas flowing above the drop can be controlled as previously described (53). First, compressed air (21% oxygen) was allowed to flow over the cell suspension until cells were equilibrated (5 min). Pure nitrogen gas, which does not affect *A. brasilense* behavior (9), was next quickly (<1 s) added to the cell suspension (air removal stimulus). After 6 min, the nitrogen gas flowing into the chamber was replaced with compressed air (air addition stimulus). The entire assay was recorded with the use of a charge-coupled-device (CCD) camera for video and motion tracking analysis. Analysis of swimming velocity was performed using CellTrak version 1.5 (Motion Analysis Corp., Santa Rosa, CA). One- to three-second segments of video were optimized to subtract background using ImageJ (http://rsb.info.nih.gov/ij/). For deter-

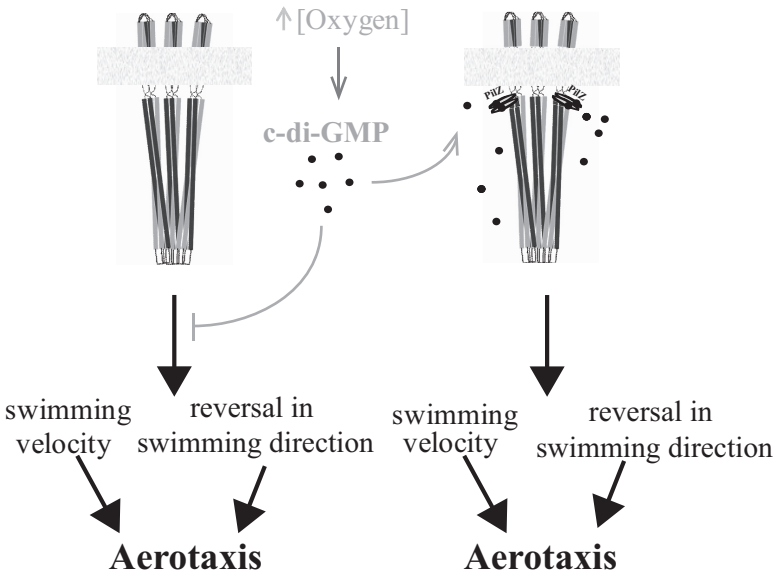

FIG 7 Model depicting the effect of c-di-GMP binding to Tlp1 on changes in swimming velocity and reversal frequency mediated by the Che pathways. The pointed arrows indicate activation, while blunt-end arrows indicate inhibition. The C-terminal PilZ domain of Tlp1 is represented as an oval. Trimers of receptor dimers are represented as simplification of chemotaxis signaling clusters. The light-gray text and arrows indicate conditions of increased aeration and intracellular c-di-GMP levels.

mination of reversal frequencies of cell suspensions, 30-frame segments (30 frames taken in 1 s) of video were analyzed using ImageJ. Individual cells visible in all frames were analyzed for changes in swimming direction. Each cell analyzed was marked (Cell Counter plugin) to ensure no duplications, and the resulting number of direction changes was recorded in Excel (Microsoft Corp., Redmond, WA). At least 100 cells were analyzed for each time point. The average reversal frequency was calculated in Excel.

Protein overexpression and purification. The DNA fragment corresponding to amino acids (aa) 344 to 660 of the wild-type Tlp1 (which encode the C-terminal MCP and PilZ domains but lack the N-terminal transmembrane and HAMP domains) was amplified and cloned into pMAL-c2x (NEB) to construct maltose binding protein (MBP) translational fusion using pMAL-Tlp-F-XbaI and pMAL-Tlp-R-HindIII (see Table S2 in the supplemental material). The R562A, R563A, R567, and N589 mutations were made via site-directed mutagenesis (QuikChange II; Stratagene) using the vector with cloned MBP-cTlp1 as the template (see Table S1). The MBP-Tlp1 fusion protein and its mutants, MBP-cTlp1^{R562A}, MBP-cTlp1$^{R562A\ R563A}$, MBP-cTlp1^{R567D}, and MBP-cTlp1^{N589A}, were overexpressed and purified, essentially as previously described (54). Protein purity was assessed by SDS-PAGE. Protein concentrations were measured with the Bradford protein assay kit (Bio-Rad).

Equilibrium dialysis. Protein-nucleotide binding was examined by equilibrium dialysis in Dispo-Biodialyzer cassettes (The Nest Group, Southborough, MA) as previously reported (21). The nucleotide concentrations were quantified by measuring peak areas of the eluted nucleotides from the HPLC column as described earlier (54). Binding constants were calculated by the GraphPad Prism software, version 5.03 (GraphPad Software, San Diego, CA), using the nonlinear regression model.

Antibody production, affinity purification, and Western blots. A C-terminal fragment of Tlp1 (aa 299 to 664) was PCR amplified from pUCTlp1 with the native stop codon and recombined into pDONR221 using BP Clonase II (Invitrogen) by using the manufacturer's protocol and sequence verified to yield pDONR*tlp*^{Cterm}. Tlp1^{Cterm} was introduced into pET-59-DEST (Novagen) using LR clonase II (Invitrogen), yielding pET-Tlp1C, and sequence verified (see Table S1 in the supplemental material). A correct clone was transformed into *E. coli* BL21(DE3) for recombinant protein expression and purification over an Ni-nitrilotriacetic acid (NTA) agarose column (Qiagen), according to the manufacturer's recommendations (Invitrogen). The affinity tags were cleaved from Tlp1^{Cterm} using thrombin (Novagen) per the manufacturer's protocol, and purified Tlp1^{Cterm} was eluted after passage through an additional Ni-NTA agarose column. Protein purity was verified by SDS-PAGE, and Tlp1^{Cterm} was sent for antibody production in rabbit (Thermo Scientific). Antisera were affinity purified using whole-cell extracts of the *tlp1* mutant conjugated to NHS-Sepharose 4B (Sigma). For Western blots, proteins from SDS-PAGE were transferred to nitrocellulose using a *trans*-blot SD semidry transfer cell (Bio-Rad) and probed with the affinity-purified anti-Tlp1^{Cterm} antiserum as a primary antibody (1:5,000) as described previously (13).

Preparation of the stable-isotope-labeled internal standard, ($^{13}C_{20}$)c-di-GMP. *E. coli* BL21(pRP87) capable of overexpressing PleD*, a constitutively active diguanylate cyclase from *Caulobacter crescentus* (55), was grown and induced in M9 medium supplemented with ^{13}C-glucose as the carbon source. This allowed purification of PleD* containing ($^{13}C_{20}$), as opposed to ($^{12}C_{20}$)c-di-GMP. Briefly, cells were inoculated into M9 medium from an overnight culture and grown to an OD_{600} of 0.5. Isopropyl-β-D-thiogalactopyranoside (IPTG) was added to a final concentration of 0.4 mM, and the cells were incubated at 22°C overnight. Cells were collected, resuspended in lysis buffer (25 mM Tris-HCl [pH 8.0], 500 mM NaCl, 10 mM imidazole) and lysed by several passages through a French press. Cell debris was removed by centrifugation at 17,000 rpm for 45 min. The supernatant was incubated with equilibrated Ni-agarose resin by batch binding at 4°C for 30 min and loaded onto a gravity column, washed thoroughly with wash buffer (lysis buffer with 30 mM imidazole), and eluted with 250 mM imidazole. The eluate was concentrated by ultrafiltration and dialyzed to remove imidazole prior to ($^{13}C_{20}$)c-di-GMP synthesis. ($^{13}C_{20}$)c-di-GMP was synthesized using ($^{13}C_{10}$)GTP (25 μM; Sigma-Aldrich) and aliquots of purified PleD* (30 μM) in synthesis buffer (75 mM Tris-HCl [pH 8], 250 mM NaCl, 25 mM KCl, and 10 mM $MgCl_2$) overnight at 25°C. Due to ($^{13}C_{20}$)c-di-GMP product inhibition of PleD activity, the enzyme was concentrated by ultrafiltration, and the supernatant containing the ($^{13}C_{20}$)c-di-GMP was collected and checked for purity via LC-MS/MS. The enzyme fraction was then resuspended in fresh synthesis buffer with an additional 25 μM ($^{13}C_{10}$)GTP to facilitate further synthesis. After overnight incubation, samples were boiled 10 min and centrifuged, and the ($^{13}C_{20}$)c-di-GMP containing supernatant was collected and analyzed. Solutions were tested for the presence of any GDP, GTP, c-di-GMP, and their corresponding ^{13}C-isotopologues via LC-MS/MS. Those that contained only ($^{13}C_{20}$)c-di-GMP were pooled and lyophilized. The powder was then resuspended in approximately 10 ml, and the final concentration was determined by measuring the absorbance of the solutions with a UV-Vis spectrometer at 254 nm and using an extinction coefficient of 26,100 M^{-1} cm^{-1} to calculate concentrations (56). The stock solution was 190 μM.

c-di-GMP extraction in a temporal assay for aerotaxis. Cultures of *A. brasilense* were grown overnight in MMAB supplemented with 5% (wt/vol) pyruvate instead of malate. Cultures were transferred to sterile medium bottles, allowing gas infusion into the media. Cultures were infused with air for several minutes to equilibrate cells. An initial 40-ml sample of cells was extracted and quickly frozen in conical tubes with liquid nitrogen (time 0). The gas was then switched to nitrogen, and three additional 40-ml samples were extracted and frozen 10, 20, and 40 s after gas switch. After 5.5 min of nitrogen infusion, a 40-ml sample was ex-

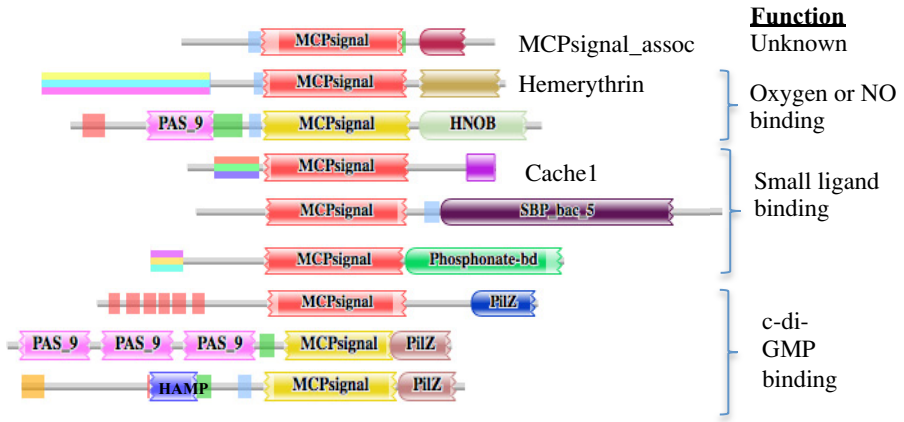

FIG 8 Domain architectures of selected chemotaxis receptor proteins containing identifiable C-terminal domains. The domains were identified using the Pfam database. MCPsignal, MCP signaling domain; MCPsignal_assoc, domain of unknown function often present downstream of MCPsignal; Cache_1 and SBP_bac, small molecule binding domain; Phosphonate_bd, phosphonate binding domain; PAS9, sensory domain possibly involved in heme binding; HAMP, signal transduction domain often found in the MCP proteins and involved in signal transduction to the MCPsignal domain.

tracted and frozen. At 6 min after initial gas switch, air was replaced with nitrogen gas and three additional samples were taken 10, 20, and 40 s after the switch and frozen. Samples were centrifuged at 6,000 rpm. The cell pellets were quickly resuspended with extraction buffer (acetonitrile-methanol-water, 40:40:20, with 0.1 M formic acid) supplemented with benzoic acid (17 μM) and ($^{13}C_{20}$)c-di-GMP (0.76 μM) and incubated on ice for 30 min. The cell extracts were centrifuged at 14,000 rpm for 15 min, and 300 μl of the supernatants was quickly transferred to an autosampler vial with 26 μl 15% ammonium carbonate.

Mass spectrometry and quantification of intracellular c-di-GMP. This metabolite was measured using a previously reported procedure with slight modifications (57). For separation of metabolites, a C_{18} stationary-phase column (150 by 2.0 mm) with a proprietary imbedded polar group was used (Synergy Hydro-RP; Phenomenex, Torrance, CA) packed with 80-Å particles with 4-μm pores and maintained at 25°C. The mobile phases consisted of solvent A, 11 mM tributylamine, and 15 mM acetic acid in 97% HPLC-grade water and 3% HPLC-grade methanol; and solvent B, HPLC-grade methanol. These solvents were used to create a 50-min gradient of the following profile: t = 0 min, 100% solvent A, 0% solvent B; t = 5 min, 100% solvent A, 0% solvent B; t = 10 min, 80% solvent A, 20% solvent B; t = 15, 80% solvent A, 20% solvent B; t = 30, 35% solvent A, 65% solvent B; t = 33, 5% solvent A, 95% solvent B; t = 37, 5% solvent A, 95% solvent B; t = 38, 100% solvent A, 0% solvent B; t = 50, 100% solvent A, 0% solvent B. The flow rate was 200 μl min^{-1}. The eluent was introduced directly into a Finnigan TSQ Quantum Discovery Max triple quadrupole mass spectrometer. Ions were detected using multiple-reaction monitoring mode. Peaks were integrated manually in Xcalibur QualBrowser, and the concentration of c-di-GMP was calculated using the following equation:

$$\frac{\text{c-di-GMP signal}}{(^{13}C_{20})\text{c-di-GMP signal}} \times \text{known } (^{13}C_{20})\text{c-di-GMP} \times \frac{1}{[\text{protein}]} \times \frac{1}{\text{volume sampled}} \times \text{volume extraction solvent} = \frac{[\text{c-di-GMP}]}{\text{Protein}}$$

SUPPLEMENTAL MATERIAL

Supplemental material for this article may be found at http://mbio.asm.org/lookup/suppl/doi:10.1128/mBio.00001-13/-/DCSupplemental.

Figure S1, PDF file, 0.4 MB.
Figure S2, PDF file, 0.5 MB.
Figure S3, PDF file, 0.6 MB.
Table S1, DOCX file, 0 MB.
Table S2, DOCX file, 0.1 MB.

ACKNOWLEDGMENTS

This work was supported by NSF MCB-1052575 to M.G. and MCB-0919819 to G.A.

We thank J.S. Parkinson and E. Maurellio for insightful comments.

REFERENCES

1. **Wadhams GH, Armitage JP.** 2004. Making sense of it all: bacterial chemotaxis. Nat. Rev. Mol. Cell. Biol. **5**:1024–1037.
2. **Buchan A, Crombie B, Alexandre GM.** 2010. Temporal dynamics and genetic diversity of chemotactic-competent microbial populations in the rhizosphere. Environ. Microbiol. **12**:3171–3184.
3. **Alexander RP, Zhulin IB.** 2007. Evolutionary genomics reveals conserved structural determinants of signaling and adaptation in microbial chemoreceptors. Proc. Natl. Acad. Sci. U. S. A. **104**:2885–2890.
4. **Hazelbauer GL, Falke JJ, Parkinson JS.** 2008. Bacterial chemoreceptors: high-performance signaling in networked arrays. Trends Biochem. Sci. **33**:9–19.
5. **Alexandre G, Greer-Phillips S, Zhulin IB.** 2004. Ecological role of energy taxis in microorganisms. FEMS Microbiol. Rev. **28**:113–126.
6. **Bible A, Russell MH, Alexandre G.** 2012. The *Azospirillum brasilense* Che1 chemotaxis pathway controls the swimming velocity which affects transient cell-to-cell clumping. J. Bacteriol. **194**:3343–3355.
7. **Wisniewski-Dyé F, Borziak K, Khalsa-Moyers G, Alexandre G, Sukharnikov LO, Wuichet K, Hurst GB, McDonald WH, Robertson JS, Barbe V, Calteau A, Rouy Z, Mangenot S, Prigent-Combaret C, Normand P, Boyer M, Siguier P, Dessaux Y, Elmerich C, Condemine G, Krishnen G, Kennedy I, Paterson AH, González V, Mavingui P, Zhulin IB.** 2011. *Azospirillum* genomes reveal transition of Bacteria from aquatic to terrestrial environments. PLoS Genet. **7**:e102430. http://dx.doi.org/10.1371/journal.pgen.1002430.
8. **Bible AN, Stephens BB, Ortega DR, Xie Z, Alexandre G.** 2008. Function of a chemotaxis-like signal transduction pathway in modulating motility, cell clumping, and cell length in the alphaproteobacterium *Azospirillum brasilense*. J. Bacteriol. **190**:6365–6375.
9. **Alexandre G, Greer SE, Zhulin IB.** 2000. Energy taxis is the dominant behavior in *Azospirillum brasilense*. J. Bacteriol. **182**:6042–6048.
10. **Zhulin IB, Bespalov VA, Johnson MS, Taylor BL.** 1996. Oxygen taxis and proton motive force in *Azospirillum brasilense*. J. Bacteriol. **178**:5199–5204.
11. **Alexandre G.** 2010. Coupling metabolism and chemotaxis-dependent behaviours by energy taxis receptors. Microbiology **156**:2283–2293.
12. **Taylor BL, Zhulin IB, Johnson MS.** 1999. Aerotaxis and other energy-sensing behavior in bacteria. Annu. Rev. Microbiol. **53**:103–128.
13. **Xie Z, Ulrich LE, Zhulin IB, Alexandre G.** 2010. PAS domain containing chemoreceptor couples dynamic changes in metabolism with chemotaxis. Proc. Natl. Acad. Sci. U. S. A. **107**:2235–2240.
14. **Greer-Phillips SE, Stephens BB, Alexandre G.** 2004. An energy taxis

transducer promotes root colonization by *Azospirillum brasilense*. J. Bacteriol. **186**:6595–6604.
15. **Amikam D, Galperin MY.** 2006. PilZ domain is part of the bacterial c-di-GMP binding protein. Bioinformatics **22**:3–6.
16. **Hengge R.** 2009. Principles of c-di-GMP signalling in bacteria. Nat. Rev. Microbiol. **7**:263–273.
17. **Mills E, Pultz IS, Kulasekara HD, Miller SI.** 2011. The bacterial second messenger c-di-GMP: mechanisms of signalling. Cell. Microbiol. **13**: 1122–1129.
18. **Schirmer T, Jenal U.** 2009. Structural and mechanistic determinants of c-di-GMP signalling. Nat. Rev. Microbiol. **7**:724–735.
19. **Carreño-López R, Sánchez A, Camargo N, Elmerich C, Baca BE.** 2009. Characterization of *chsA*, a new gene controlling the chemotactic response in *Azospirillum brasilense* Sp7. Arch. Microbiol. **191**:501–507.
20. **Pellequer JL, Brudler R, Getzoff ED.** 1999. Biological sensors: more than one way to sense oxygen. Curr. Biol. **9**:R416–R418.
21. **Ryjenkov DA, Simm R, Römling U, Gomelsky M.** 2006. The PilZ domain is a receptor for the second messenger c-di-GMP. The PilZ domain protein YcgR controls motility in enterobacteria. J. Biol. Chem. **281**: 30310–30314.
22. **Ko J, Ryu KS, Kim H, Shin JS, Lee JO, Cheong C, Choi BS.** 2010. Structure of PP4397 reveals the molecular basis for different c-di-GMP Binding modes by Pilz domain proteins. J. Mol. Biol. **398**:97–110.
23. **Taylor BL, Watts KJ, Johnson MS.** 2007. Oxygen and redox sensing by two-component systems that regulate behavioral responses: behavioral assays and structural studies of Aer using *in vivo* disulfide cross-linking. Methods Enzymol. **422**:190–232.
24. **Szurmant H, Ordal GW.** 2004. Diversity in chemotaxis mechanisms among the *Bacteria* and *Archaea*. Microbiol. Mol. Biol. Rev. **68**:301–319.
25. **Benach J, Swaminathan SS, Tamayo R, Handelman SK, Folta-Stogniew E, Ramos JE, Forouhar F, Neely H, Seetharaman J, Camilli A, Hunt JF.** 2007. The structural basis of cyclic diguanylate signal transduction by PilZ domains. EMBO J. **26**:5153–5166.
26. **Shin JS, Ryu KS, Ko J, Lee A, Choi BS.** 2011. Structural characterization reveals that a PilZ domain protein undergoes substantial conformational change upon binding to cyclic dimeric guanosine monophosphate. Protein Sci. **20**:270–277.
27. **Massazza DA, Parkinson JS, Studdert CA.** 2011. Cross-linking evidence for motional constraints within chemoreceptor trimers of dimers. Biochemistry **50**:820–827.
28. **Hu W.** 2011. A possible degree of motional freedom in bacterial chemoreceptor cytoplasmic domains and its potential role in signal transduction. Int. J. Biochem. Mol. Biol. **2**:99–110.
29. **Ames P, Studdert CA, Reiser RH, Parkinson JS.** 2002. Collaborative signaling by mixed chemoreceptor teams in *Escherichia coli*. Proc. Natl. Acad. Sci. U. S. A. **99**:7060–7065.
30. **Ames P, Parkinson JS.** 2006. Conformational suppression of intermolecular receptor signaling defects. Proc. Natl. Acad. Sci. U. S. A. **103**:9292–9297.
31. **Briegel A, Li X, Bilwes AM, Hughes KT, Jensen GJ, Crane BR.** 2012. Bacterial chemoreceptor arrays are hexagonally packed trimers of receptor dimers networked by rings of kinase and coupling proteins. Proc. Natl. Acad. Sci. U. S. A. **109**:3766–3771.
32. **Briegel A, Ortega DR, Tocheva EI, Wuichet K, Li Z, Chen S, Müller A, Iancu CV, Murphy GE, Dobro MJ, Zhulin IB, Jensen GJ.** 2009. Universal architecture of bacterial chemoreceptor arrays. Proc. Natl. Acad. Sci. U. S. A. **106**:17181–17186.
33. **Lai WC, Beel BD, Hazelbauer GL.** 2006. Adaptational modification and ligand occupancy have opposite effects on positioning of the transmembrane signalling helix of a chemoreceptor. Mol. Microbiol. **61**:1081–1090.
34. **Stephens BB, Loar SN, Alexandre G.** 2006. Role of CheB and CheR in the complex chemotactic and aerotactic pathway of *Azospirillum brasilense*. J. Bacteriol. **188**:4759–4768.
35. **Bibikov SI, Miller AC, Gosink KK, Parkinson JS.** 2004. Methylation-independent aerotaxis mediated by the *Escherichia coli* Aer protein. J. Bacteriol. **186**:3730–3737.
36. **Zhulin IB, Armitage JP.** 1993. Motility, chemokinesis, and methylation-independent chemotaxis in *Azospirillum brasilense*. J. Bacteriol. **175**: 952–958.
37. **Zimmer MA, Szurmant H, Saulmon MM, Collins MA, Bant JS, Ordal GW.** 2002. The role of heterologous receptors in McpB-mediated signalling in *Bacillus subtilis* chemotaxis. Mol. Microbiol. **45**:555–568.
38. **Ames P, Parkinson JS.** 1988. Transmembrane signaling by bacterial chemoreceptors: *E. coli* transducers with locked signal output. Cell **55**: 817–826.
39. **Dang CV, Niwano M, Ryu J, Taylor BL.** 1986. Inversion of aerotactic response in *Escherichia coli* deficient in CheB protein methylesterase. J. Bacteriol. **166**:275–280.
40. **Bespalov VA, Zhulin IB, Taylor BL.** 1996. Behavioral responses of *Escherichia coli* to changes in redox potential. Proc. Natl. Acad. Sci. U. S. A. **93**:10084–10089.
41. **Endres RG, Wingreen NS.** 2006. Precise adaptation in bacterial chemotaxis through "assistance neighborhoods." Proc. Natl. Acad. Sci. U. S. A. **103**:13040–13044.
42. **Levit MN, Grebe TW, Stock JB.** 2002. Organization of the receptor-kinase signaling array that regulates *Escherichia coli* chemotaxis. J. Biol. Chem. **277**:36748–36754.
43. **Li M, Hazelbauer GL.** 2005. Adaptational assistance in clusters of bacterial chemoreceptors. Mol. Microbiol. **56**:1617–1626.
44. **Fang X, Gomelsky M.** 2010. A post-translational, c-di-GMP-dependent mechanism regulating flagellar motility. Mol. Microbiol. **76**:1295–1305.
45. **Paul K, Nieto V, Carlquist WC, Blair DF, Harshey RM.** 2010. The c-di-GMP binding protein YcgR controls flagellar motor direction and speed to affect chemotaxis by a "backstop brake" mechanism. Mol. Cell **38**:128–139.
46. **Boehm A, Kaiser M, Li H, Spangler C, Kasper CA, Ackermann M, Kaever V, Sourjik V, Roth V, Jenal U.** 2010. Second messenger-mediated adjustment of bacterial swimming velocity. Cell **141**:107–116.
47. **Christen M, Kulasekara HD, Christen B, Kulasekara BR, Hoffman LR, Miller SI.** 2010. Asymmetrical distribution of the second messenger c-di-GMP upon bacterial cell Division. Science **328**:1295–1297.
48. **Finn RD, Mistry J, Tate J, Coggill P, Heger A, Pollington JE, Gavin OL, Gunasekaran P, Ceric G, Forslund K, Holm L, Sonnhammer EL, Eddy SR, Bateman A.** 2010. The Pfam protein families database. Nucleic Acids Res. **38**:D211–D222.
49. **Vanstockem M, Michiels K, Vanderleyden J, Van Gool AP.** 1987. Transposon mutagenesis of *Azospirillum brasilense* and *Azospirillum lipoferum*: physical analysis of Tn*5* and Tn*5-mob* insertion mutants. Appl. Environ. Microbiol. **53**:410–415.
50. **Siuti P, Green C, Edwards AN, Doktycz MJ, Alexandre G.** 2011. The chemotaxis-like Che1 pathway has an indirect role in adhesive cell properties of *Azospirillum brasilense*. FEMS Microbiol. Lett. **323**:105–112.
51. **Keen NT, Tamaki S, Kobayashi D, Trollinger D.** 1988. Improved broad-host-range plasmids for DNA cloning in Gram-negative bacteria. Gene **70**:191–197.
52. **Figurski DH, Helinski DR.** 1979. Replication of an origin-containing derivative of plasmid RK2 dependent on a plasmid function provided in *trans*. Proc. Natl. Acad. Sci. U. S. A. **76**:1648–1652.
53. **Laszlo DJ, Taylor BL.** 1981. Aerotaxis in *Salmonella typhimurium*: role of electron transport. J. Bacteriol. **145**:990–1001.
54. **Ryjenkov DA, Tarutina M, Moskvin OV, Gomelsky M.** 2005. Cyclic diguanylate is a ubiquitous signaling molecule in bacteria: insights into biochemistry of the GGDEF protein domain. J. Bacteriol. **187**:1792–1798.
55. **Paul R, Weiser S, Amiot NC, Chan C, Schirmer T, Giese B, Jenal U.** 2004. Cell cycle-dependent dynamic localization of a bacterial response regulator with a novel di-guanylate cyclase output domain. Genes Dev. **18**:715–727.
56. **Zhang Z, Gaffney BL, Jones RA.** 2004. c-di-GMP displays a monovalent metal ion-dependent polymorphism. J. Am. Chem. Soc. **126**: 16700–16701.
57. **Waters CM, Lu W, Rabinowitz JD, Bassler BL.** 2008. Quorum sensing controls biofilm formation in *Vibrio cholerae* through modulation of cyclic di-GMP levels and repression of *vpsT*. J. Bacteriol. **190**:2527–2536.
58. **O'Toole GA, Kolter R.** 1998. Initiation of biofilm formation in *Pseudomonas fluorescens* WCS365 proceeds via multiple, convergent signalling pathways: a genetic analysis. Mol. Microbiol. **28**:449–461.